Machine Learning Tries for Photonics

IA et Sciences Physiques @ AMU

2023-11-22 Julien Wojak (*et al*)

IF is not IA

IF is not IA

Institut Fresnel

IF is not IA

Everybody knows

Institut Fresnel

IF is a Physics lab

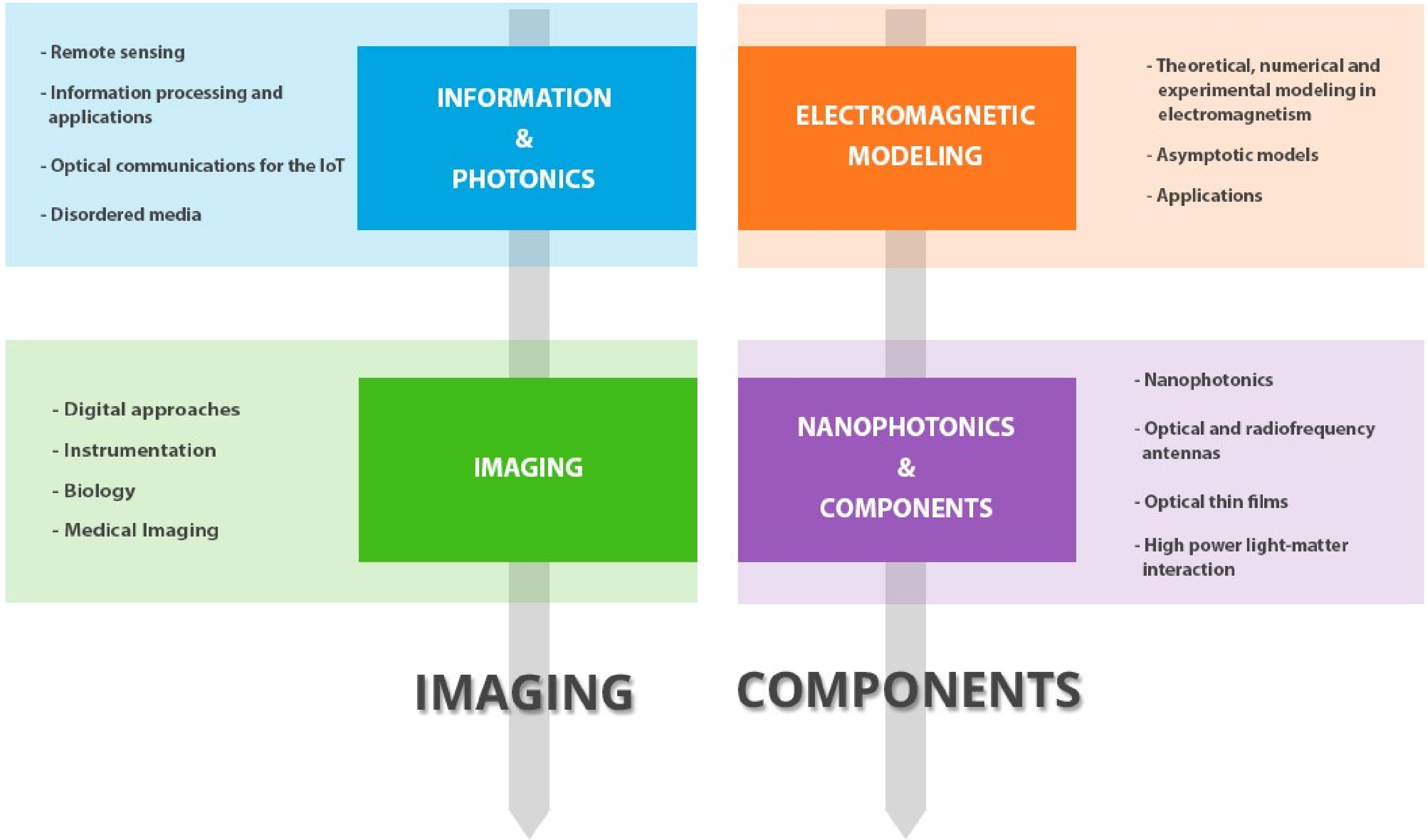

IF is a Physics lab using IA

I] Classical Image Processing Problems

→ detection
→ segmentation
→ denoising (image restoration)

II] Mapping Problems

→ synthetics CT
→ synthetics SHG/TPFE

III] Inverse problems

→ Multi-layer design

IF is a physics lab using IA

I] Classical Image Processing Problems

→ **detection**

→ **segmentation**

→ **denoising (image restoration)**

II] Mapping Problems

→ synthetics CT

→ synthetics SHG/TPFE

III] Inverse problems

→ Multi-layer design

Image Processing – **Detection/Segmentation/Quantification**

Segmentation : delineation of objects in images

→ pre-processing step
→ get objects features
→ quantification on measurements

medical images (MRI, Laser images….)

→ Organs
→ laser damage
→ cells..

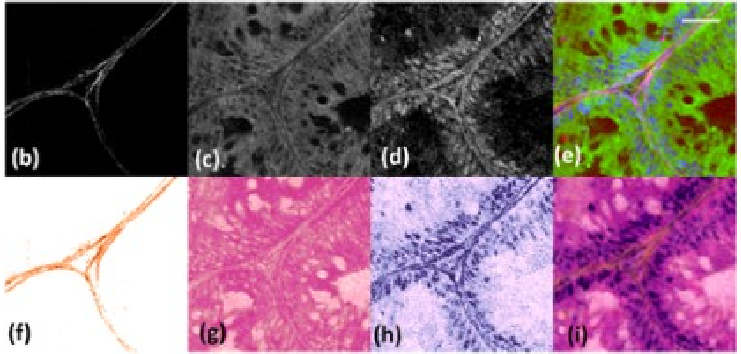

(2019) 9:10052 | https://doi.org/10.1038/s41598-019-46489-x

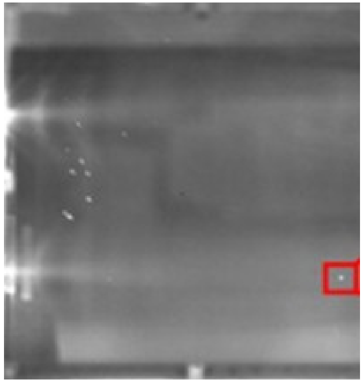

1084-7529/22/101881-12 2022

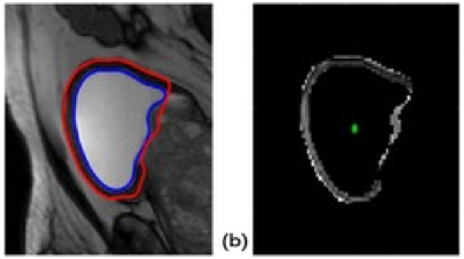

https://doi.org/10.3390/jimaging8060151

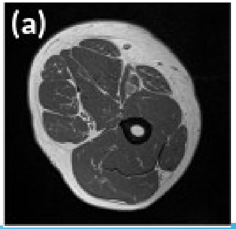

Segmentation : delineation of objects in images

→ pre-processing step

→ get objects features

→ quantification on measurements

=> Standard AI task

→ two examples of our work

+ *bounding box for damages detection/quantification*

+ *segmentation of muscle in MRI for fat fraction quantification*

Image Processing – Detection/Segmentation/Quantification

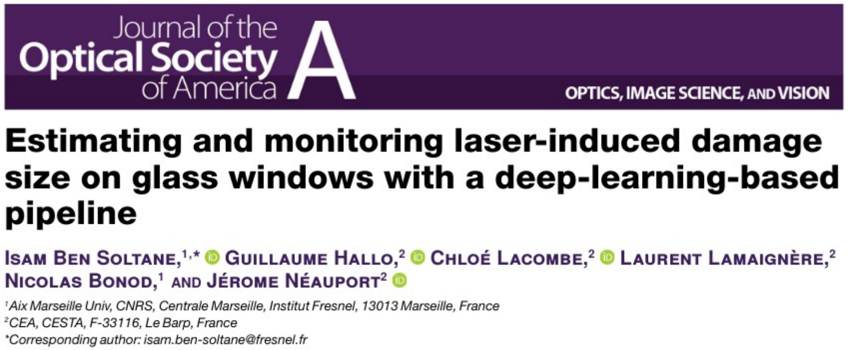
Journal of the Optical Society of America A
OPTICS, IMAGE SCIENCE, AND VISION

Estimating and monitoring laser-induced damage size on glass windows with a deep-learning-based pipeline

Isam Ben Soltane,[1,*] Guillaume Hallo,[2] Chloé Lacombe,[2] Laurent Lamaignère,[2] Nicolas Bonod,[1] and Jérome Néauport[2]

[1]Aix Marseille Univ, CNRS, Centrale Marseille, Institut Fresnel, 13013 Marseille, France
[2]CEA, CESTA, F-33116, Le Barp, France
*Corresponding author: isam.ben-soltane@fresnel.fr

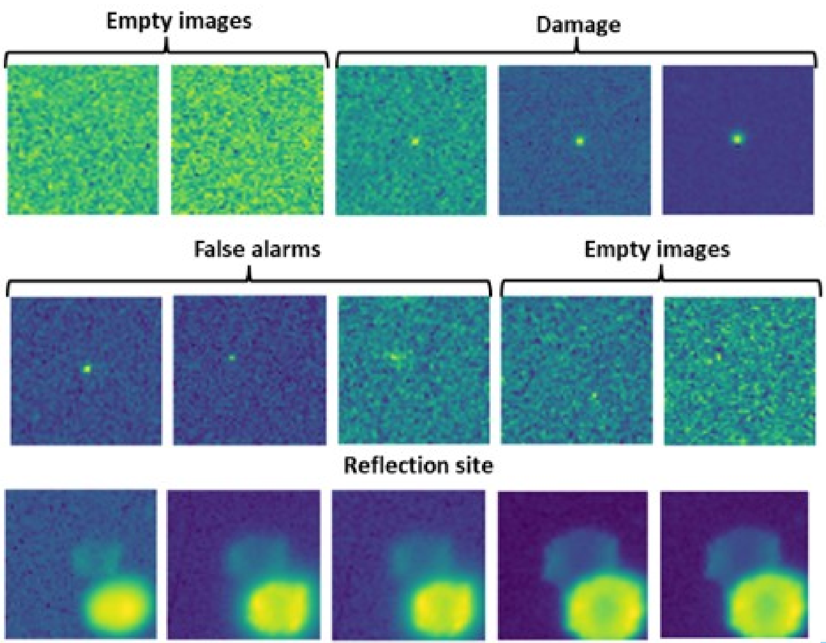

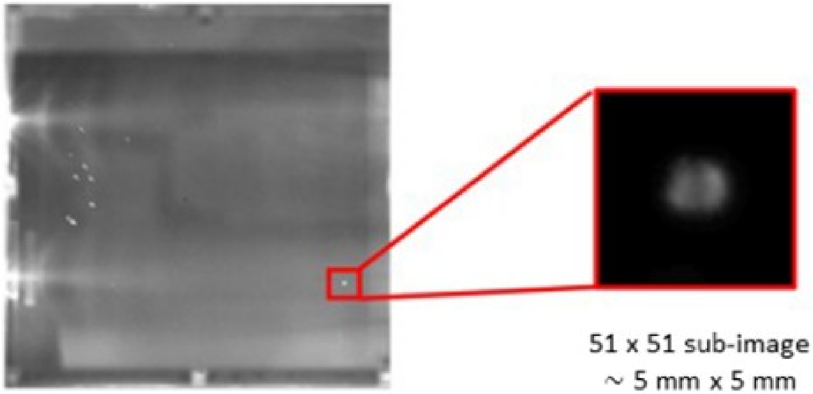

GOAL : find bounding box of damages to estimate their sizes

3 steps algorithm
- empty images detection
- reflection site detection
- damage segmentation and bounding box estimation

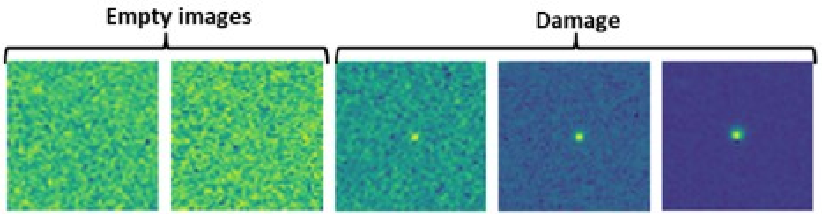

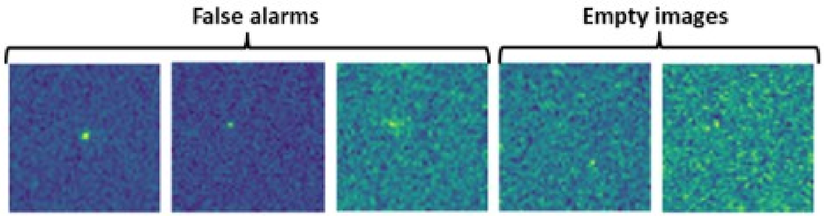

4 layers CNN

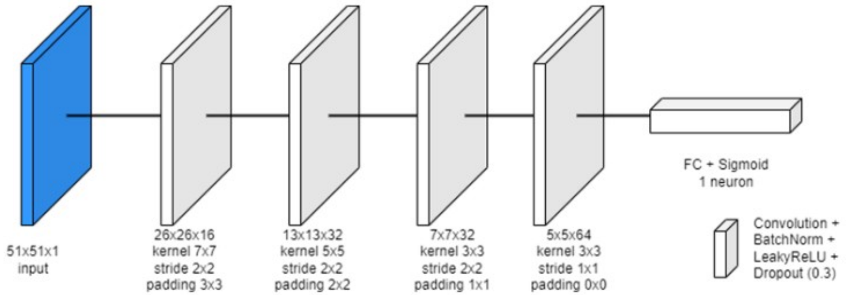

11620 sub-images of 51 × 51 pixels:
- training set : 7000 images
- validation set : 2100 images

=> Precision 95,4 %

Damage segmentation : **U-Net**

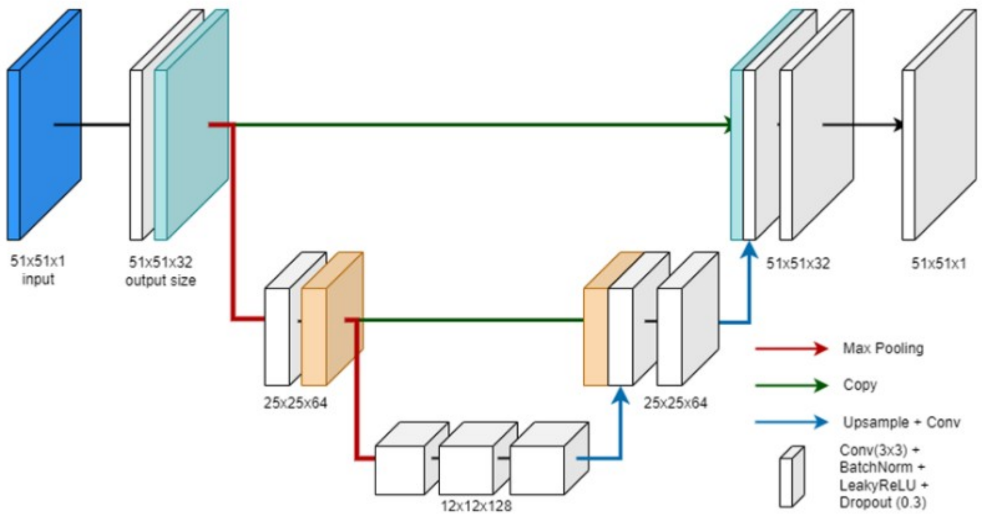

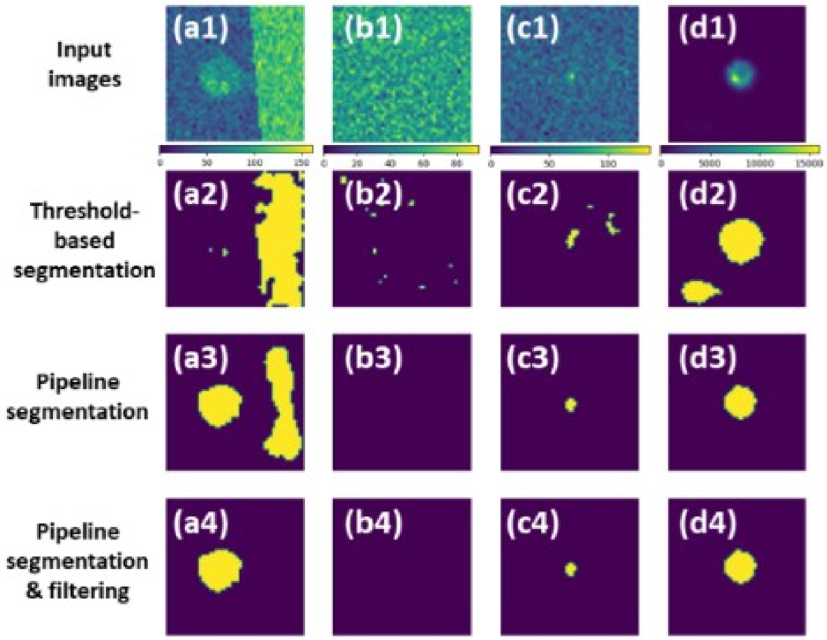

Bounding box estimation :

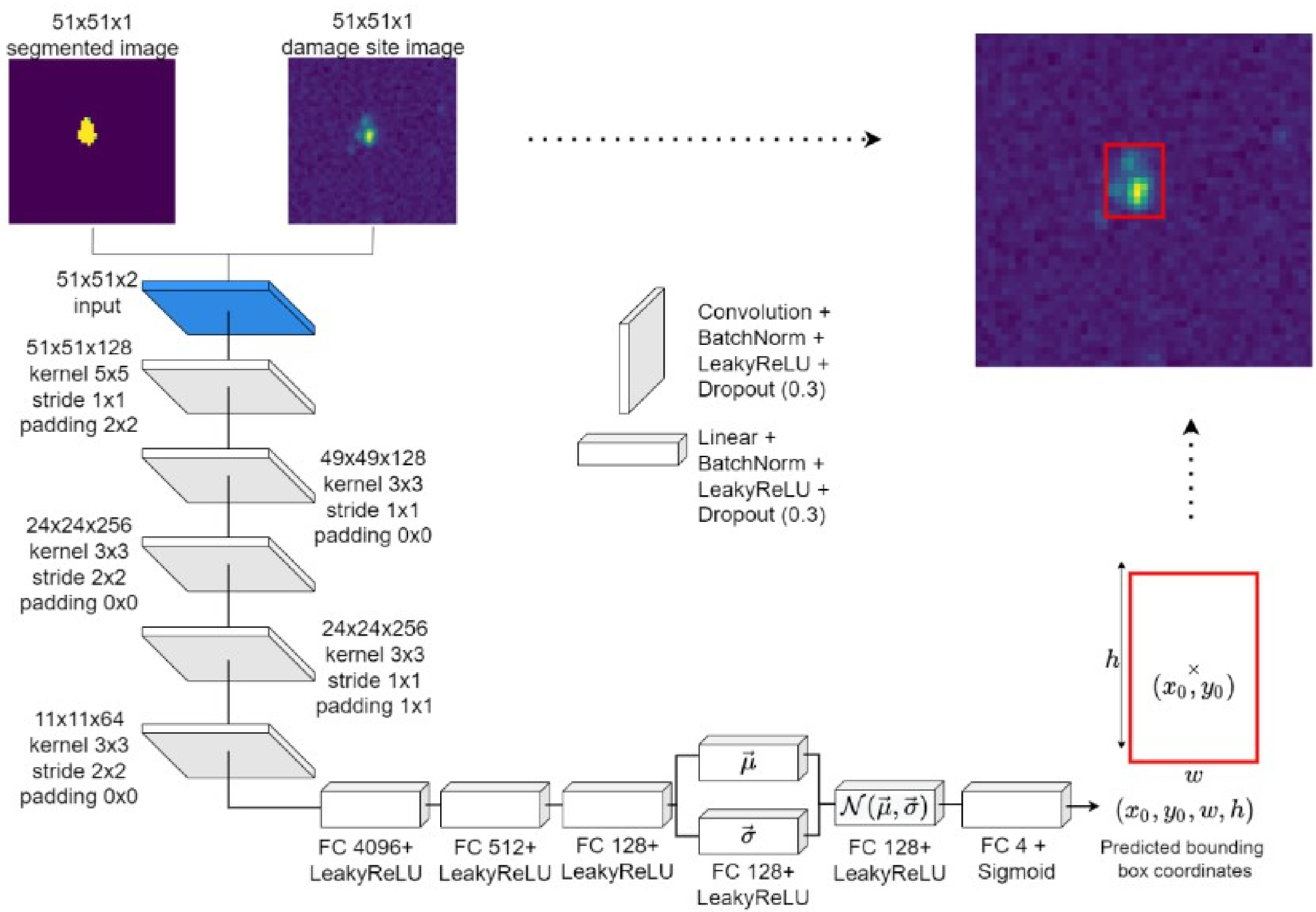

Image Processing – Detection/Segmentation/Quantification

Bounding box estimation :

Table 1. Mean Values of the Intersection over Union and Generalized Intersection over Union Calculated for the Pipeline and the Six Alternatives: Single-Step Convolutional Neural Network, ResNet50 with a Variational Neural Network as Decoder, Inception V3 with a VNN, ResNet50 with the Random Forest Algorithm as Decoder, Inception V3 with the RF, and the Random Forest Only[a, b]

	Pipeline	CNN	RN50 + VNN	IV3 + VNN	RN50 + RF	IV3 + RF	RF
IoU	0.910	0.724	0.516	0.502	0.444	0.463	0.111
GIoU	0.908	0.715	0.489	0.463	0.364	0.417	−0.398
pr	0.940	0.883	0.830	0.719	0.618	0.612	0.189
rec	0.966	0.817	0.581	0.643	0.576	0.686	0.195

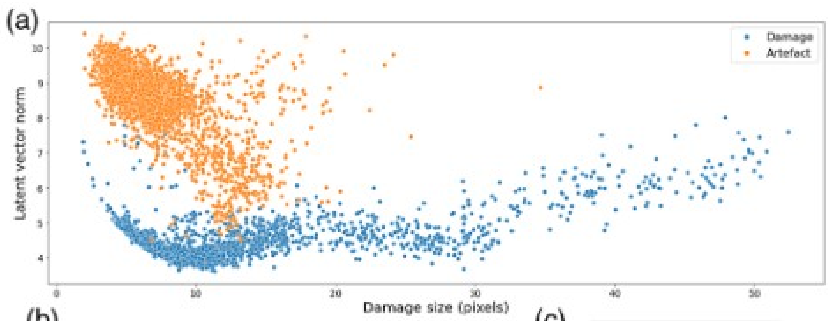

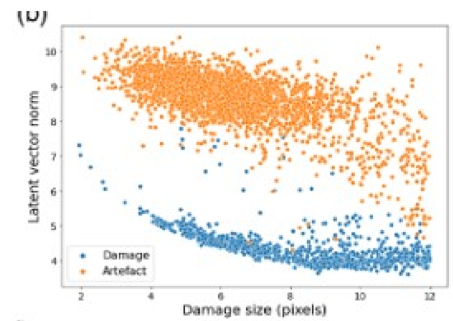

SPIE. MEDICAL IMAGING

Implementation of deep learning algorithms for automatic MRI segmentation and fat fraction quantification in individual muscles

Sandra Martin, Amira Trabelsi, Rémi Andre, Julien Wojak, Etienne Fortanier, Shahram Attatian, Maxime Guye, Marc Dubois, Redha Abdeddaim, David Bendahan

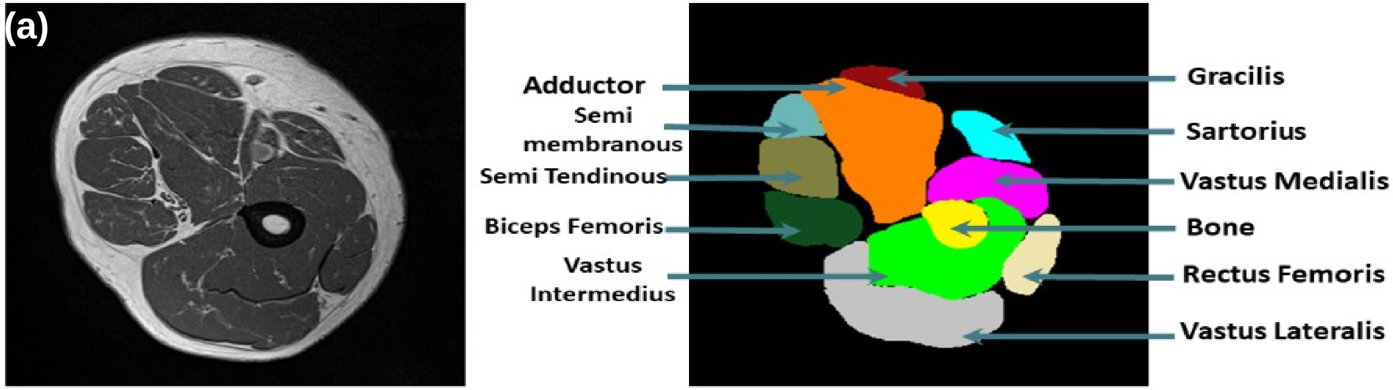

T1w MR images

Segmentation Mask

Image Processing – **Detection/Segmentation/Quantification**

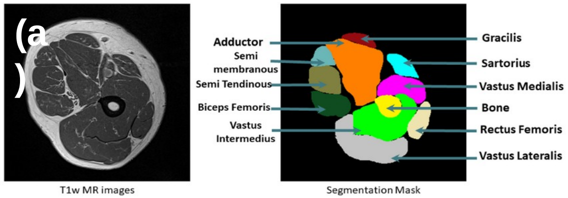

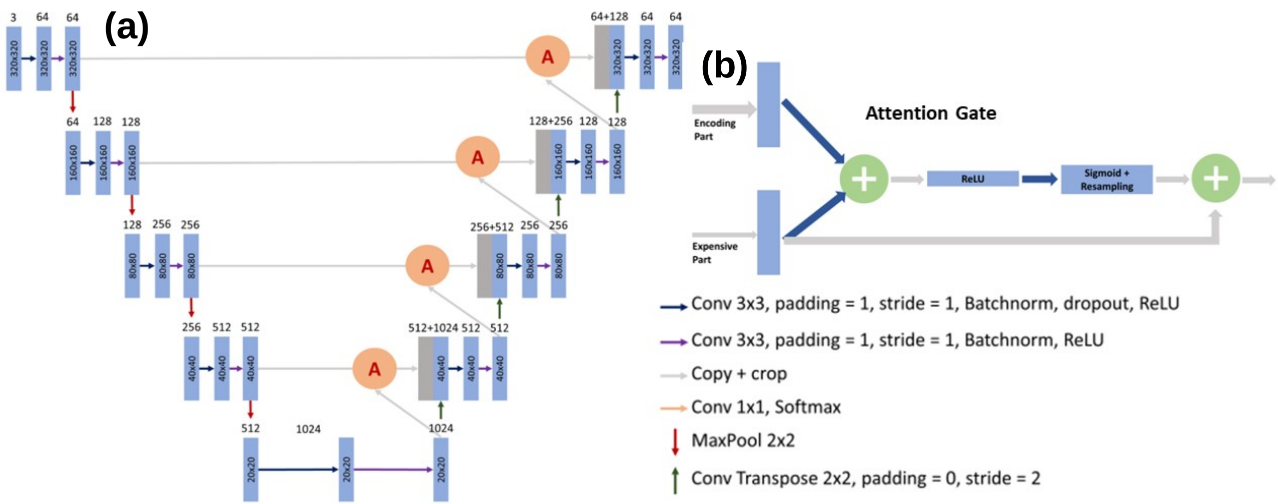

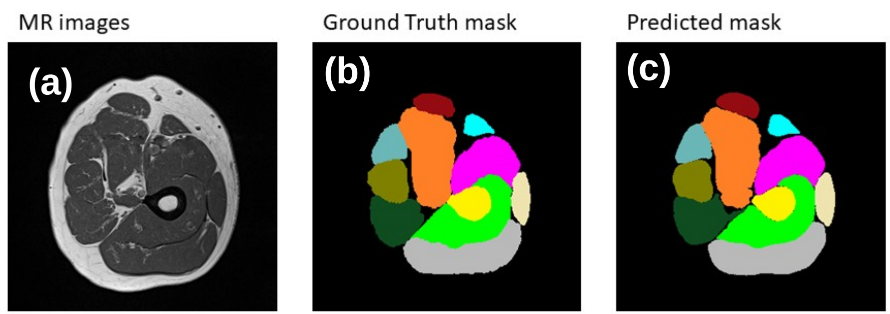

Image Processing – **Detection/Segmentation/Quantification**

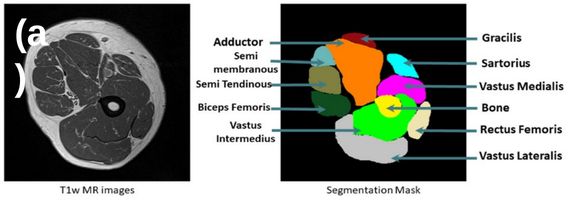

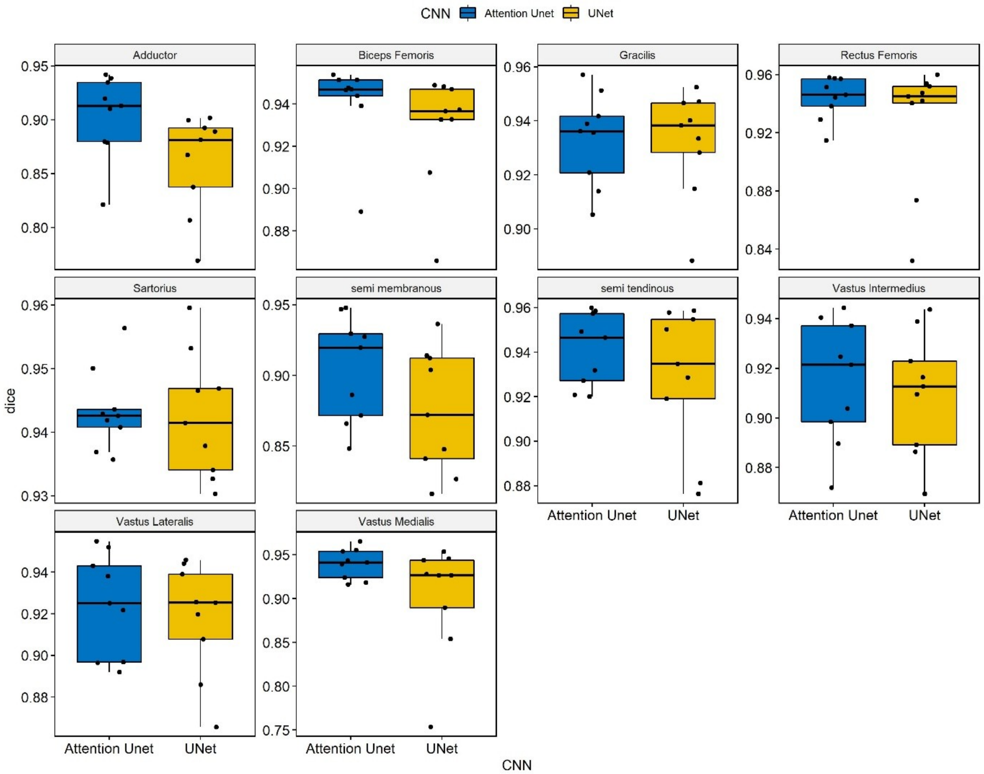

Attention U-Net	GT	U-Net	Attention U-Net	GT	U-Net
	Adductor			**Biceps Femoris**	
0.083 ± 0.03	0.089 ± 0.034	0.029 ± 0.012	0.077±0.022	0.079±0.028	0.074±0.022
	Gracilis			**Rectus Femoris**	
0.108±0.0187	0.114±0.0256	0.105±0.018	0.078±0.019	0.086±0.019	0.081±0.019
	Sartorius			**Semi Membranous**	
0.118±0.0183	0.125±0.0242	0.118±0.017	0.087±0.037	0.091±0.040	0.087±0.037
	Semi tendinous			**Vastus Intermedius**	
0.075±0.0237	0.081±0.0269	0.075±0.025	0.068±0.034	0.068±0.034	0.067±0.035
0.075±0.0223	0.076±0.0264	0.076±0.022	0.055±0.025	0.051±0.025	0.053±0.023

Results are presented as means ± SD.

IMPROVING IMAGE QUALITY IN LOW-FIELD MRI WITH DEEP LEARNING

Armando Garcia Hernandez[1], Pierre Fau[2], Stanislas Rapacchi[3], Julien Wojak[1], Hugues Mailleux[2], Mohamed Benkreira[2], Mouloud Adel[1]

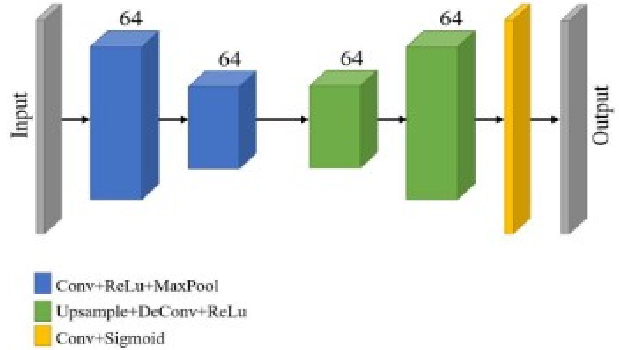

Low Field MRI : poor SNR

=> Need image restoration or denoising algo.

Tries using denoising auto-encoder

1.5 T

0.35 T

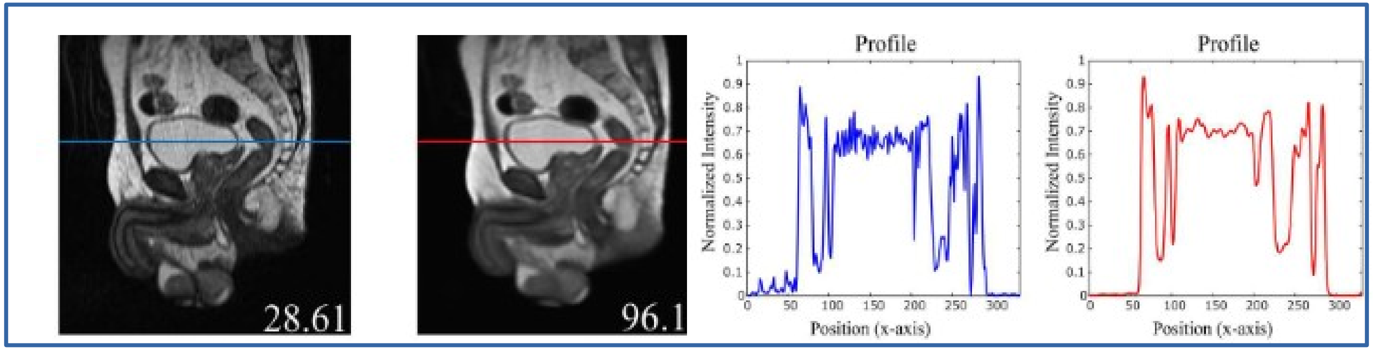

Multi-view Separable Pyramid Network for AD Prediction at MCI Stage by ^{18}F-FDG Brain PET Imaging

Xiaoxi Pan, Trong Le-Phan, Mouloud Adel, Caroline Fossati, Thierry Gaidon, Julien Wojak, and Eric Guedj, for Alzheimer's Disease Neuroimaging Initiative

IEEE Transactions on Medical Imaging, 2021, 40 (1), pp.81-92. ?10.1109/TMI.2020.3022591?. ?hal-03627176?

PET images

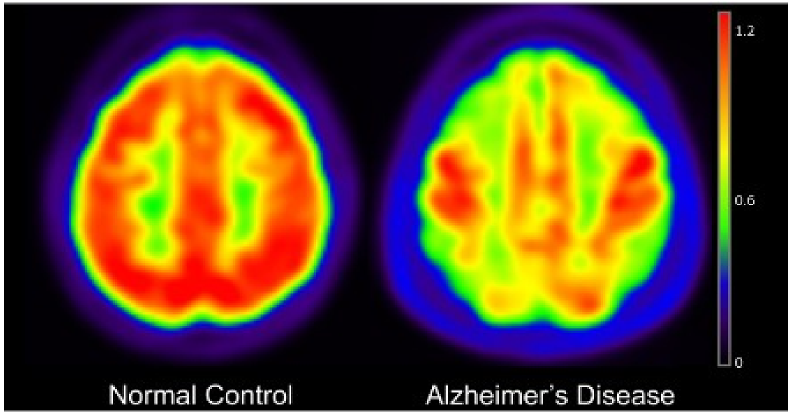

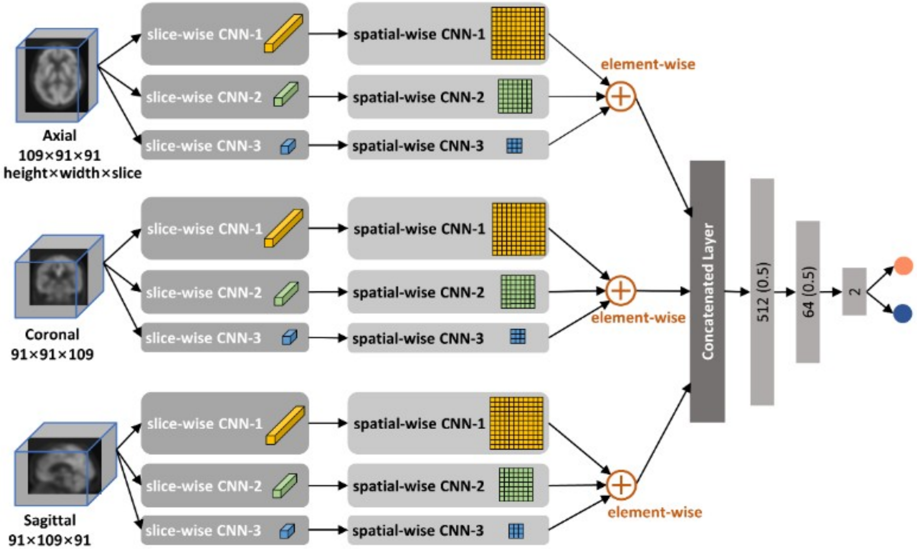

Multi-view Separable Pyramid Network for AD Prediction at MCI Stage by ^{18}F-FDG Brain PET Imaging

Xiaoxi Pan, Trong Le-Phan, Mouloud Adel, Caroline Fossati, Thierry Gaidon, Julien Wojak, and Eric Guedj, for Alzheimer's Disease Neuroimaging Initiative

IEEE Transactions on Medical Imaging, 2021, 40 (1), pp.81-92. ?10.1109/TMI.2020.3022591?. ?hal-03627176?

COMPARISON WITH BASELINE METHODS FOR AD VS. NC(%)

Methods	ACC	SEN	SPE	AUC	Parameters
Voxel-wise	92.83	**91.90**	93.71	**97.17**	–
ROI-wise	88.56	87.08	90.00	94.91	–
2D CNN	80.31	70.41	90.07	87.30	2.79 M
3D CNN	86.56	80.41	92.58	94.08	11.30 M
MiSePyNet	**93.13**	90.32	**95.49**	97.11	**1.05 M**

PERFORMANCE OF DIFFERENT VIEWS OF NETWORKS FOR PMCI VS. SMCI(%)

Views	ACC	SEN	SPE	AUC
Axial view network	**81.90**	**69.70**	**87.50**	**87.07**
Coronal view network	80.95	66.67	**87.50**	86.32
Sagittal view network	80.00	**69.70**	84.72	86.45
MiSePyNet	**83.81**	**75.76**	**87.50**	**88.89**

COMPARISON WITH BASELINE METHODS FOR FOR PMCI VS. SMCI(%)

Methods	ACC	SEN	SPE	AUC	Parameters
Voxel-wise	74.38	54.59	83.67	78.11	–
ROI-wise	75.00	55.83	83.77	78.37	–
2D CNN	72.29	48.79	83.06	76.37	2.79 M
3D CNN	78.67	55.45	**89.31**	81.91	11.30 M
MiSePyNet	**83.05**	**72.12**	88.06	**86.80**	**1.05 M**

Multi-view Separable Pyramid Network for AD Prediction at MCI Stage by ^{18}F-FDG Brain PET Imaging

Xiaoxi Pan, Trong Le-Phan, Mouloud Adel, Caroline Fossati, Thierry Gaidon, Julien Wojak, and Eric Guedj, for Alzheimer's Disease Neuroimaging Initiative

IEEE Transactions on Medical Imaging, 2021, 40 (1), pp.81-92. ?10.1109/TMI.2020.3022591?. ?hal-03627176?

PERFORMANCE COMPARISON WITH STATE-OF-THE-ART METHODS FOR pMCI VS. sMCI(%)

Category	Method	Data type	Subjects	ACC	SEN	SPE	AUC
Conventional methods	Gray *et al.* [9]	^{18}F-FDG PET	53pMCI + 64sMCI	63.1	52.2	73.2	– –
	Zhu *et al.* 2014 [11]	MRI, ^{18}F-FDG PET, CSF	43pMCI + 56sMCI	70.9	42.7	94.1	77.4
	Zhu *et al.* 2016 [12]	MRI, ^{18}F-FDG PET	43pMCI + 56sMCI	69.9	– –	– –	– –
	Cheng *et al.* [14]	MRI, ^{18}F-FDG PET, CSF	43pMCI + 56sMCI	71.6	76.4	67.9	74.1
	Pan *et al.* 2019a [15]	^{18}F-FDG PET	166pMCI + 360sMCI	79.43	69.14	84.16	83.88
	Pan *et al.* 2019b [16]	^{18}F-FDG PET	166pMCI + 360sMCI	**80.48**	65.04	**87.95**	**85.67**
Emerging methods	Lu *et al.* [26]	^{18}F-FDG PET	112pMCI + 409sMCI	82.51	**81.36**	82.85	– –
	Suk *et al.* [27]	MRI, ^{18}F-FDG PET	76pMCI + 128sMCI	70.75	25.45	**96.55**	72.15
	Yee *et al.* [32]	^{18}F-FDG PET	210pMCI + 427sMCI	74.7	74.0	75.0	81.1
	MiSePyNet (Ours)	^{18}F-FDG PET	166pMCI + 360sMCI	**83.05**	72.12	88.06	**86.80**

Partial conclusion :

- image processing problems are common in optics labs
- AI in the broadest sense addresses these problems
- **deep learning** is mature enough to handle a large number of image processing problems
- main challenges : datasets, comparison

- where is Physics ?

IF is a physics lab using IA

I] Classical Image Processing Problems
→ detection
→ segmentation
→ denoising (image restoration)

II] Mapping Problems
→ **synthetics CT**
→ **synthetics SHG/TPFE**

III] Inverse problems
→ Multi-layer design

Mapping

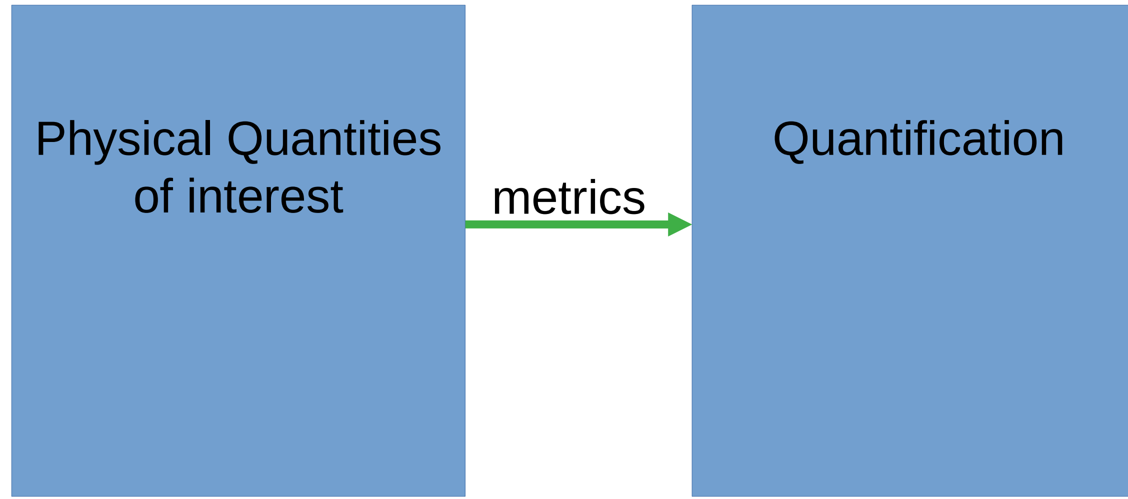

Mapping

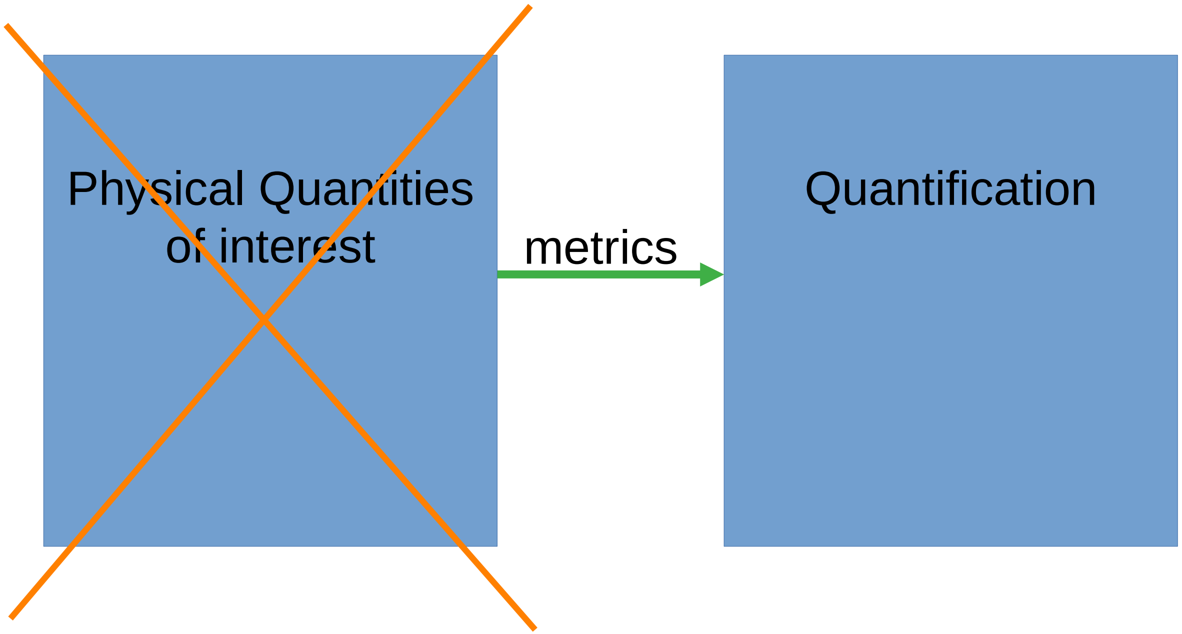

Mapping

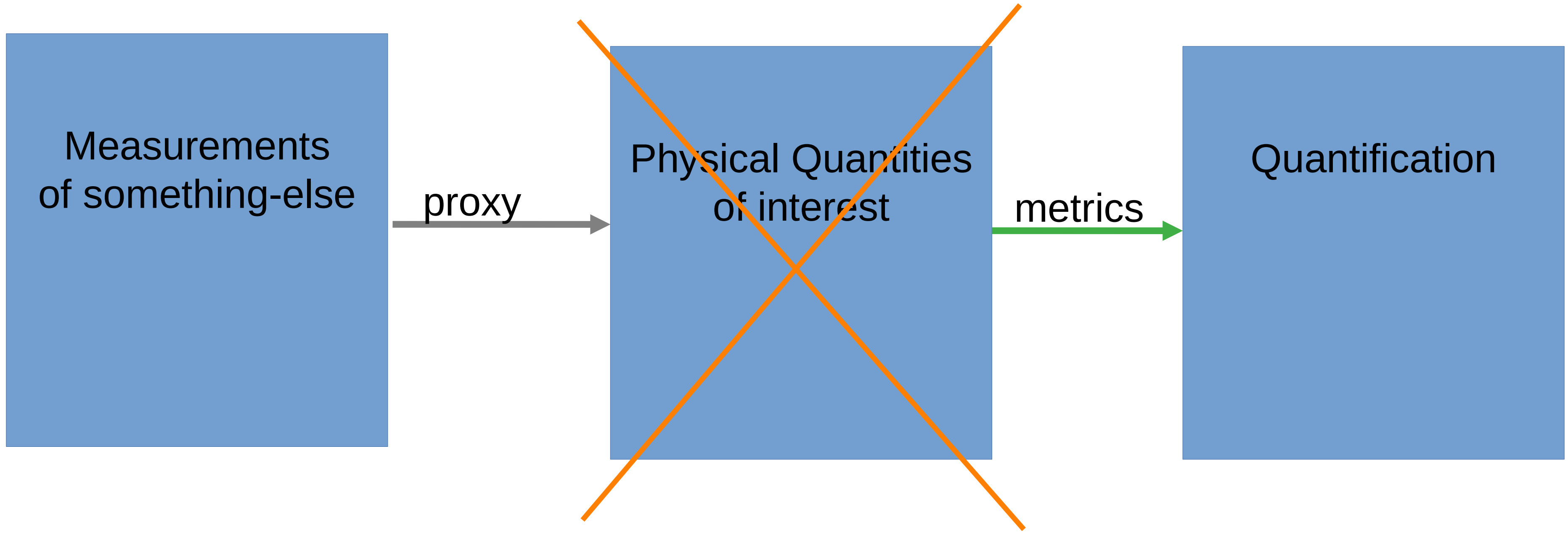
Measurements
of something-else
proxy
Physical Quantities
of interest
metrics
Quantification

Mapping

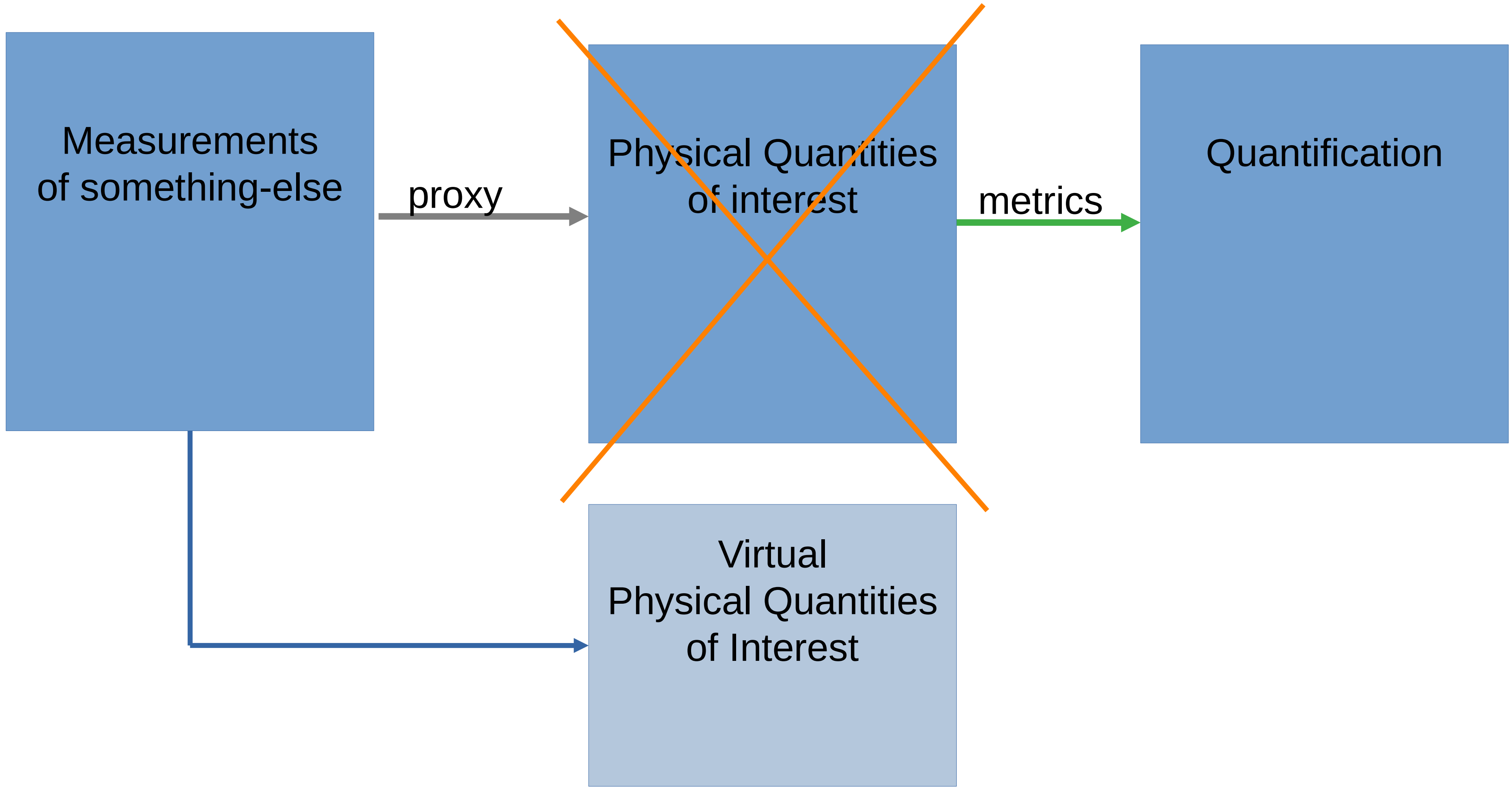

Measurements
of something-else
proxy
Physical Quantities
of interest
metrics
Quantification
Virtual
Physical Quantities
of Interest

Mapping

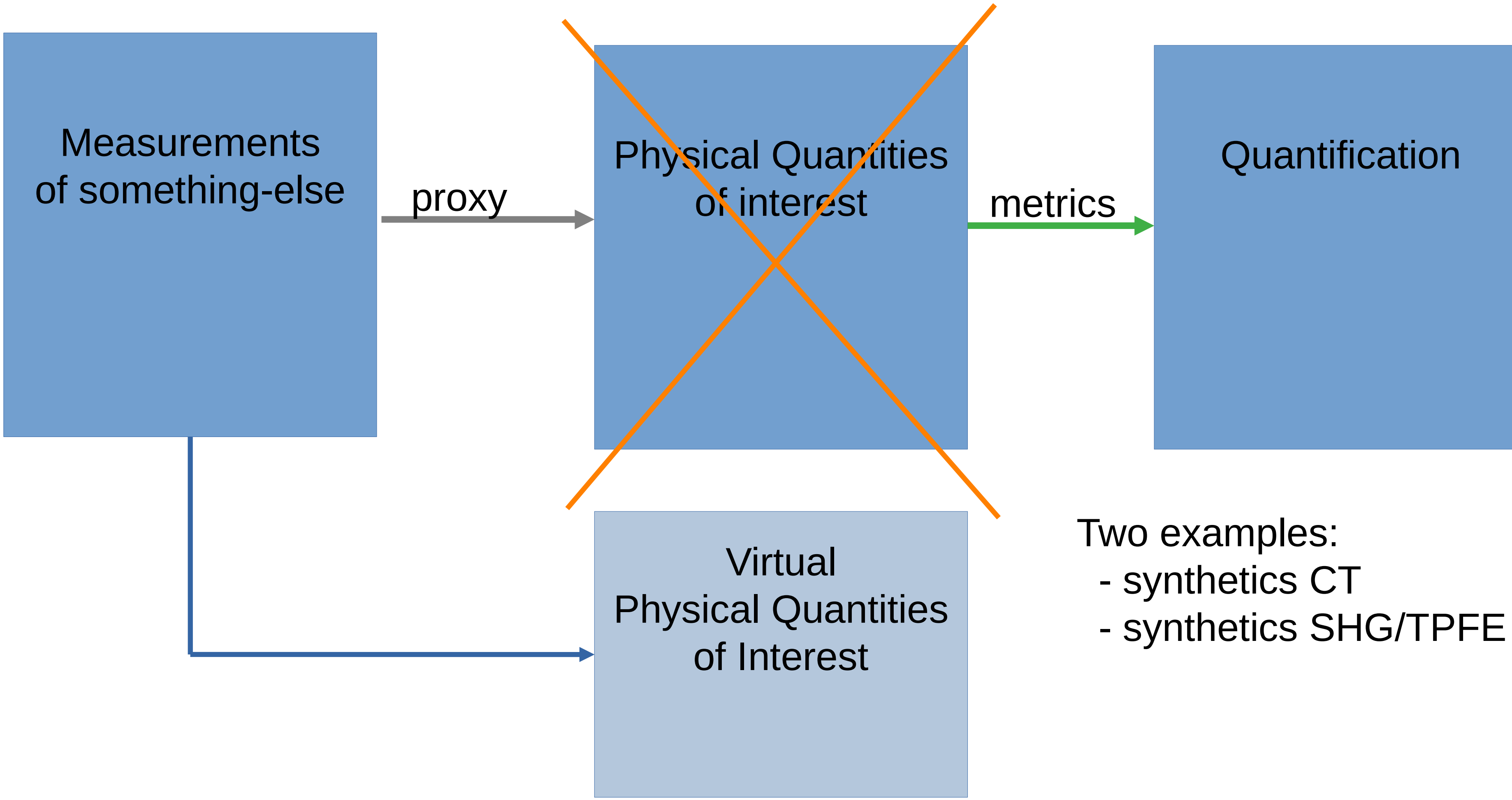

Two examples:
- synthetics CT
- synthetics SHG/TPFE

Mapping – Synthetics CT

Contents lists available at ScienceDirect

Physics and Imaging in Radiation Oncology

journal homepage: www.sciencedirect.com/journal/physics-and-imaging-in-radiation-oncology

Original Research Article

Synthetic computed tomography generation for abdominal adaptive radiotherapy using low-field magnetic resonance imaging

Armando Garcia Hernandez [a,*], Pierre Fau [b], Julien Wojak [a], Hugues Mailleux [b], Mohamed Benkreira [b], Stanislas Rapacchi [c], Mouloud Adel [a]

Radiotherapy

CT scan : dose computation

MRI : target delineation

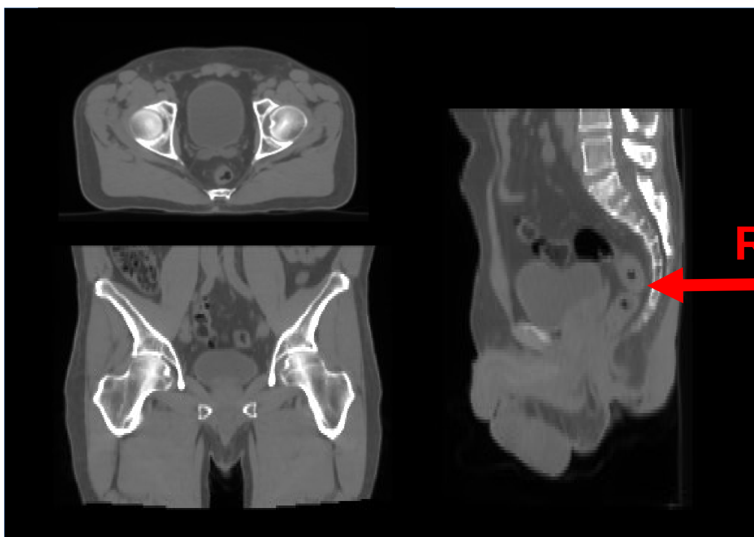

Registration

Mapping – Synthetics CT

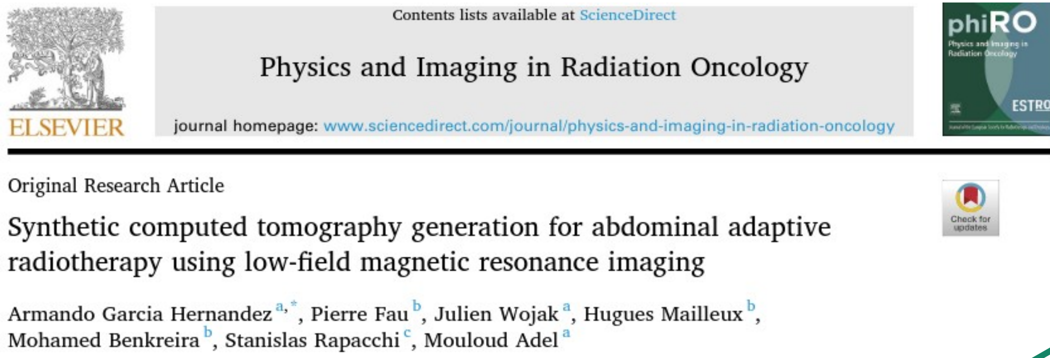
Contents lists available at ScienceDirect

Physics and Imaging in Radiation Oncology

journal homepage: www.sciencedirect.com/journal/physics-and-imaging-in-radiation-oncology

Original Research Article

Synthetic computed tomography generation for abdominal adaptive radiotherapy using low-field magnetic resonance imaging

Armando Garcia Hernandez [a,*], Pierre Fau [b], Julien Wojak [a], Hugues Mailleux [b], Mohamed Benkreira [b], Stanislas Rapacchi [c], Mouloud Adel [a]

Radiotherapy

MRLinac

CT scan : dose computation

MRI : target delineation

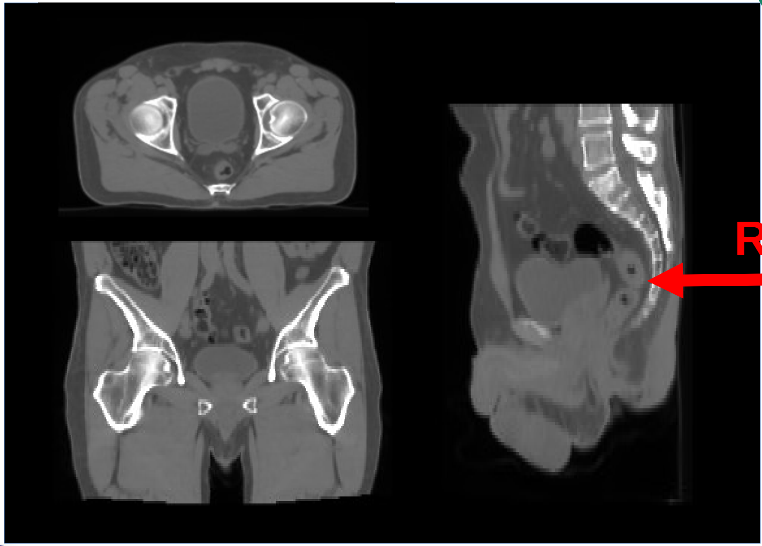

Registration

Mapping – **Synthetics CT**

Contents lists available at ScienceDirect
Physics and Imaging in Radiation Oncology
journal homepage: www.sciencedirect.com/journal/physics-and-imaging-in-radiation-oncology

Original Research Article

Synthetic computed tomography generation for abdominal adaptive radiotherapy using low-field magnetic resonance imaging

Armando Garcia Hernandez [a,*], Pierre Fau [b], Julien Wojak [a], Hugues Mailleux [b], Mohamed Benkreira [b], Stanislas Rapacchi [c], Mouloud Adel [a]

Synthetics CT generation ?

Radiotherapy

MRLinac

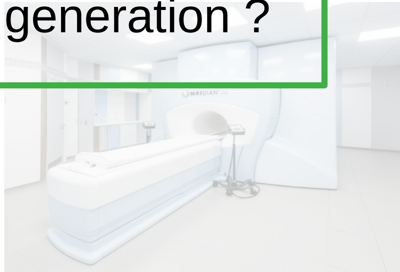

CT scan : dose computation

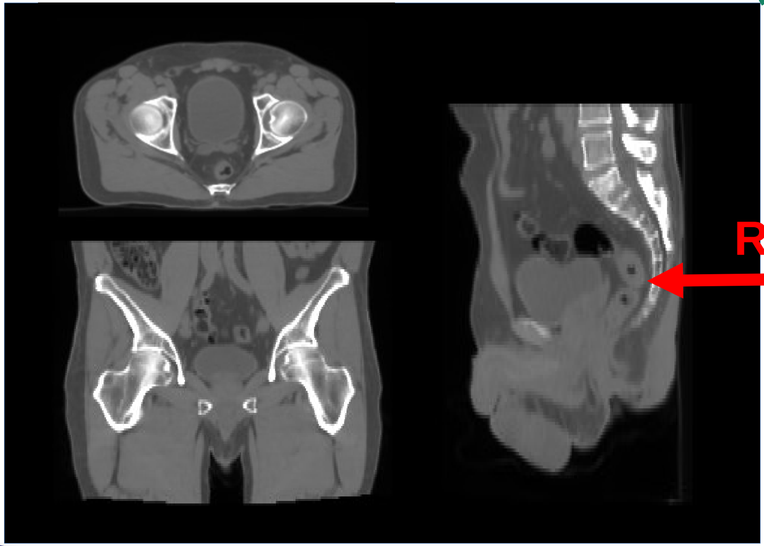

Registration

MRI : target delineation

Mapping – **Synthetics CT**

Contents lists available at ScienceDirect

Physics and Imaging in Radiation Oncology

journal homepage: www.sciencedirect.com/journal/physics-and-imaging-in-radiation-oncology

Original Research Article

Synthetic computed tomography generation for abdominal adaptive

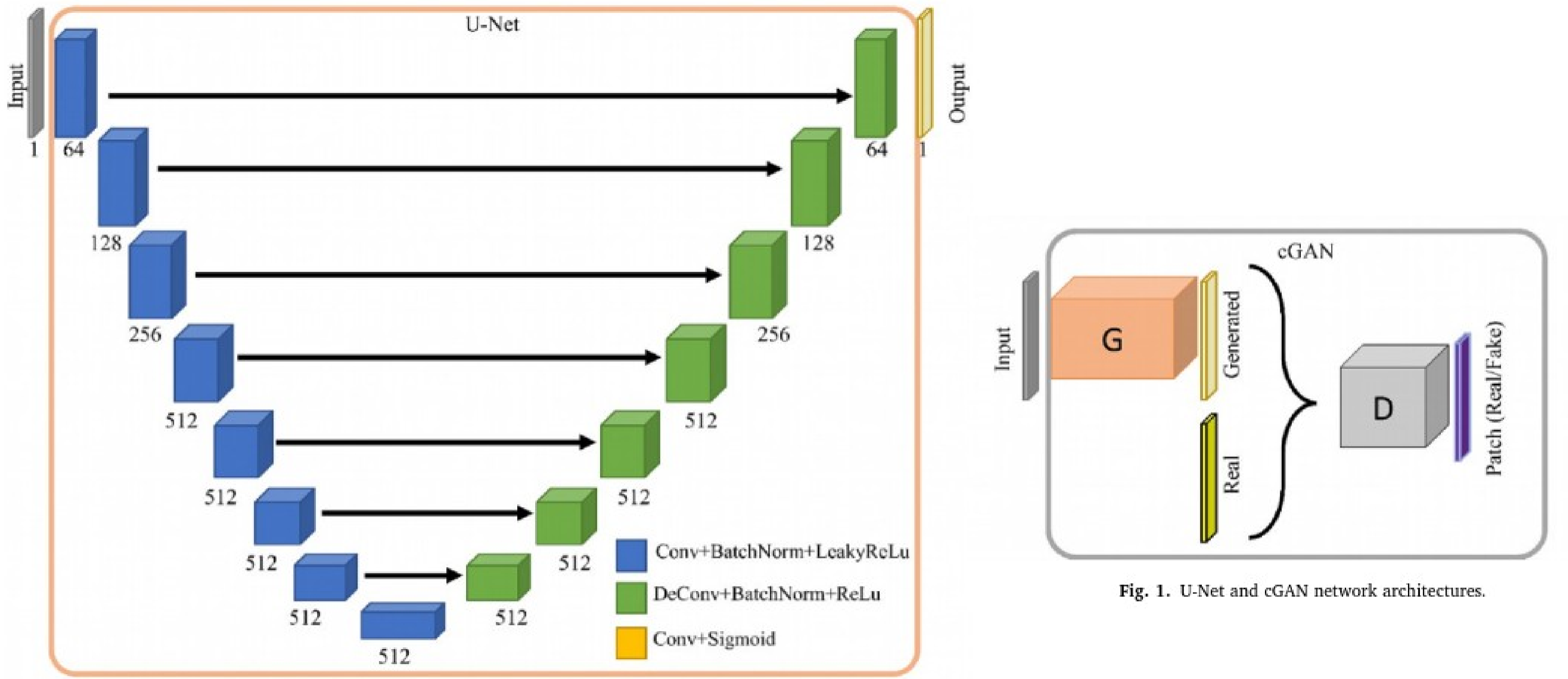

Fig. 1. U-Net and cGAN network architectures.

Mapping – **Synthetics CT**

ELSEVIER

Contents lists available at ScienceDirect

Physics and Imaging in Radiation Oncology

journal homepage: www.sciencedirect.com/journal/physics-and-imaging-in-radiation-oncology

phiRO Physics and Imaging in Radiation Oncology ESTRO

Original Research Article

Synthetic computed tomography generation for abdominal adaptive radiotherapy using low-field magnetic resonance imaging

Armando Garcia Hernandez[a,*], Pierre Fau[b], Julien Wojak[a], Hugues Mailleux[b], Mohamed Benkreira[b], Stanislas Rapacchi[c], Mouloud Adel[a]

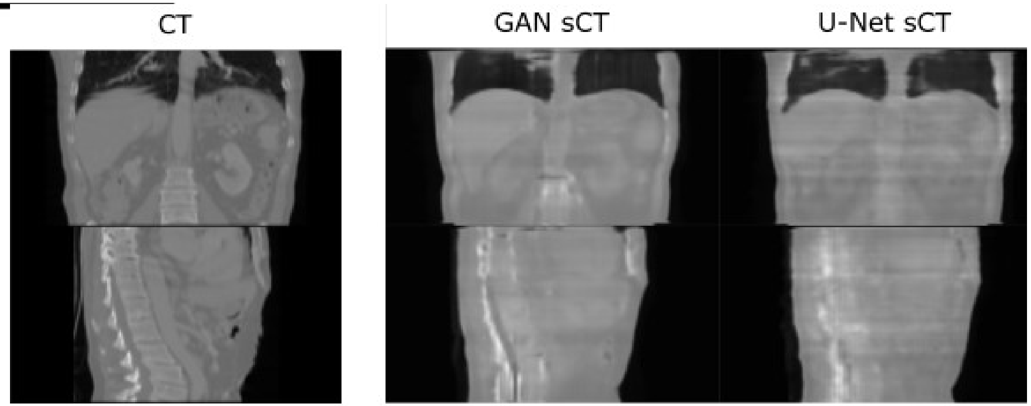

Table 3
Mean difference (%) of PTV, Liver and Stomach DVH parameters for the generated image RT plans with respect to the reference plan. Mean ± SD.

		U-Net sCT	P-values	GAN sCT	P-values	U-Net SsCT	P-values	GAN SsCT	P-values
PTV	D98	0.8 ± 1.12	<0.001	1.3 ± 0.77	0.007	1.9 ± 1.21	0.021	4.1 ± 3.27	0.109
	D50	0.8 ± 1.41	0.010	1.6 ± 0.82	0.055	2.3 ± 1.29	0.102	4.7 ± 3.59	0.172
	D2	−0.08 ± 1.68	0.035	1.3 ± 1.15	0.119	2.3 ± 1.32	0.199	4.7 ± 3.59	0.154
LIVER	D98	−0.02 ± 0.11	<0.001	−0.03 ± 0.10	<0.001	−0.05 ± 0.09	<0.001	−0.03 ± 0.10	<0.001
	D50	0.2 ± 0.61	0.211	0.2 ± 0.62	0.208	0.2 ± 0.64	0.225	0.3 ± 0.80	0.256
	D2	0.7 ± 1.35	0.401	1.1 ± 0.89	0.335	1.4 ± 1.03	0.399	3 ± 3.02	0.334
STOMACH	D98	−0.1 ± 0.28	<0.001	−0.1 ± 0.28	<0.001	−0.1 ± 0.28	<0.001	−0.1 ± 0.25	<0.001
	D50	0.4 ± 0.95	0.318	0.5 ± 0.97	0.327	0.5 ± 0.97	0.334	0.9 ± 1.55	0.338
	D2	−0.02 ± 0.11	<0.001	0.7 ± 1.23	0.347	1.1 ± 1.45	0.386	2.4 ± 2.96	0.427

Mapping – **Synthetics SHG/TPFE**

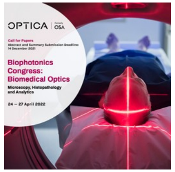

An efficient deep learning segmentation scheme for cervical collagen and elastin quantification in Mueller matrix polarimetry microscopic images

Nelson Gary, Vinh Nguyen Du Le, Julien Wojak, Mouloud Adel, Jessica Ramella-Roman, and Anabela Da Silva

- **Optical modalities** ideally suited to monitor the growth and remodeling process in the cervix: sensitive to the molecular content of the tissues, non-invasive &non-ionizing
- **Mueller Matrix** (**MM**) imaging sensitive to tissue composition and structure, non contact, can be wide field but *low sensitivity to elastin*
- **Non linear** microscopy techniques (Second Harmonic Generation (SHG), Two Photon Excitation Fluorescence (TPFE)) : highly sensitive but *invasive*

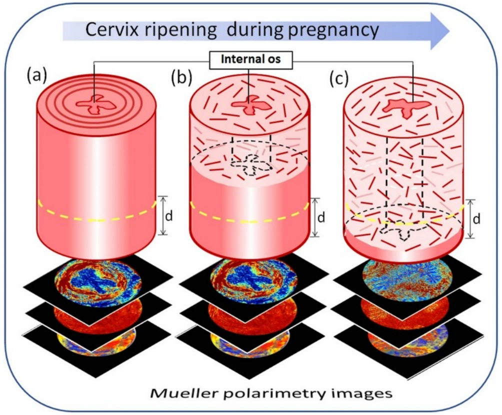

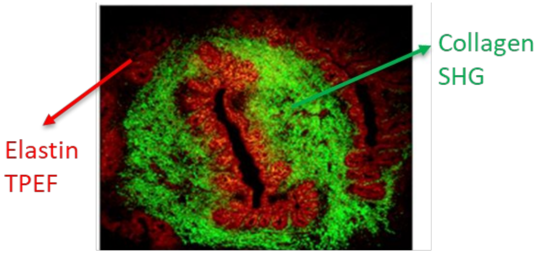

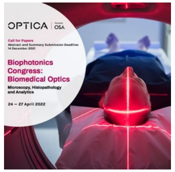

An efficient deep learning segmentation scheme for cervical collagen and elastin quantification in Mueller matrix polarimetry microscopic images

Nelson Gary, Vinh Nguyen Du Le, Julien Wojak, Mouloud Adel, Jessica Ramella-Roman, and Anabela Da Silva

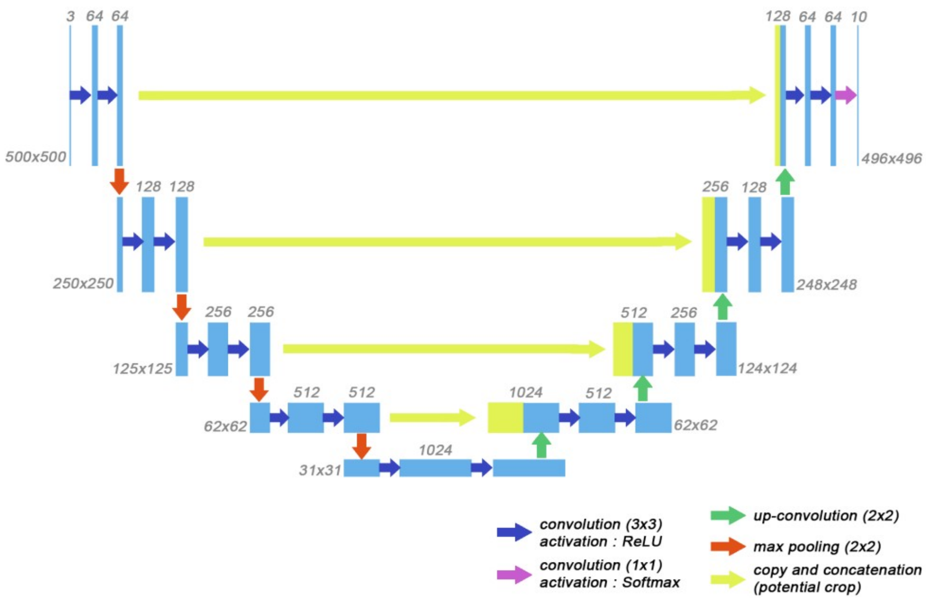

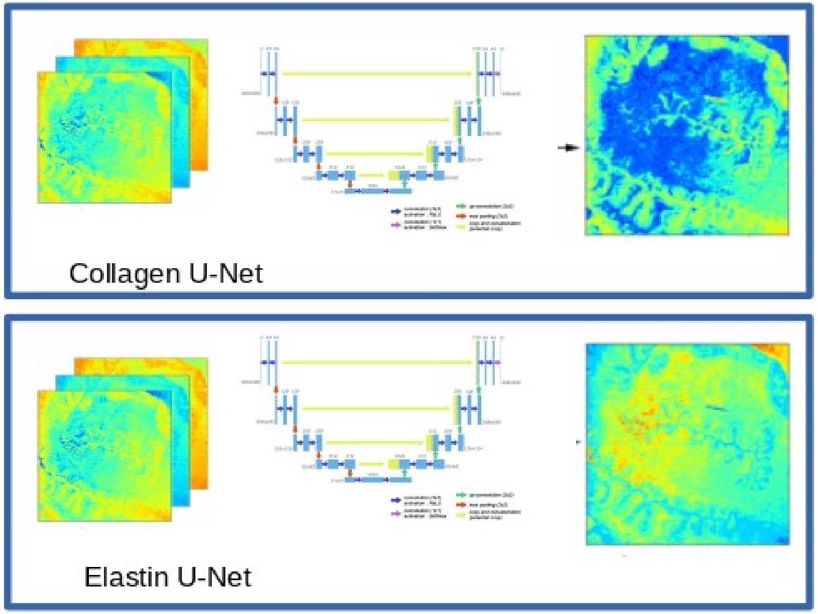

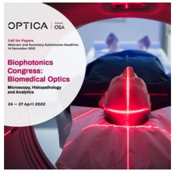

An efficient deep learning segmentation scheme for cervical collagen and elastin quantification in Mueller matrix polarimetry microscopic images

Nelson Gary, Vinh Nguyen Du Le, Julien Wojak, Mouloud Adel, Jessica Ramella-Roman, and Anabela Da Silva

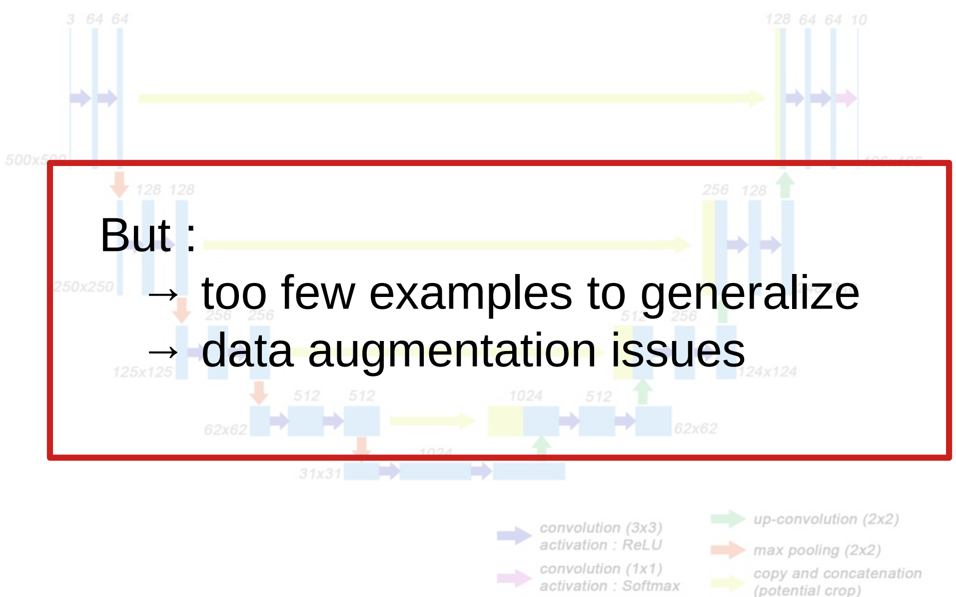

But :

→ too few examples to generalize

→ data augmentation issues

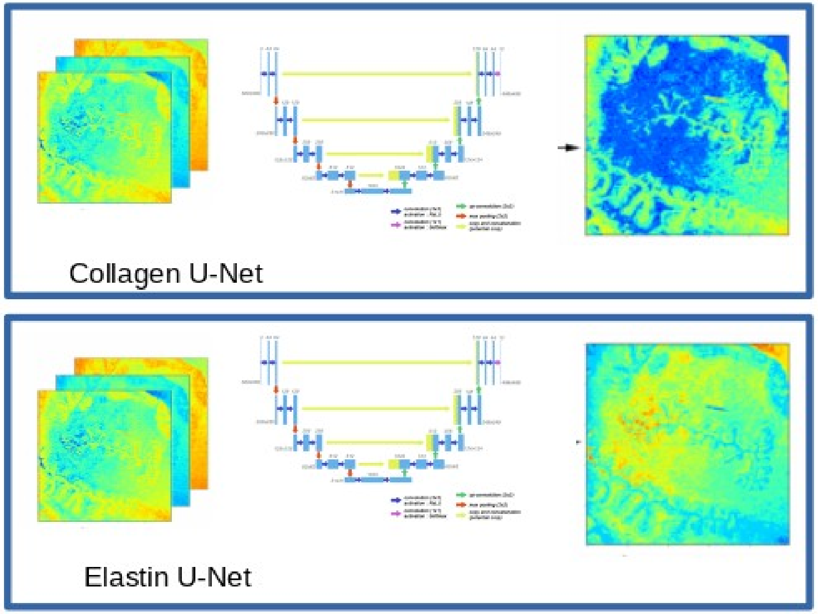

Partial conclusion :

- Mapping problems are seen as image to image mapping
- Main challenges : datasets, comparison
- Physics is in the target but not in the model

IF is a physics lab using IA

I] Classical Image Processing Problems
→ detection
→ segmentation
→ denoising (image restoration)

II] Mapping Problems
→ synthetics CT
→ synthetics SHG/TPFE

III] Inverse problems
→ **Multi-layer design**

Optics EXPRESS

Design of multilayer optical thin-films based on light scattering properties and using deep neural networks

MARIN FOUCHIER,[1,2,*] MYRIAM ZERRAD,[1] MICHEL LEQUIME,[1] AND CLAUDE AMRA[1]

[1] *Aix Marseille Univ, CNRS, Centrale Marseille, Institut Fresnel, Marseille, France*
[2] *Centre National d'Etudes Spatiales, Toulouse, France*
[*] *marin.fouchier@fresnel.fr*

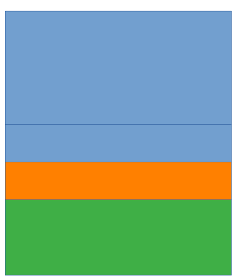

Multilayer optical thin film

Direct model

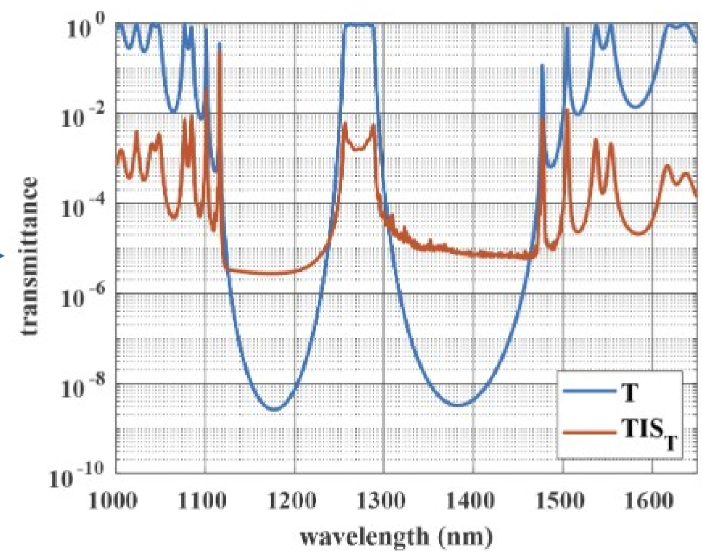

Inverse Problems – **multi-layer design**

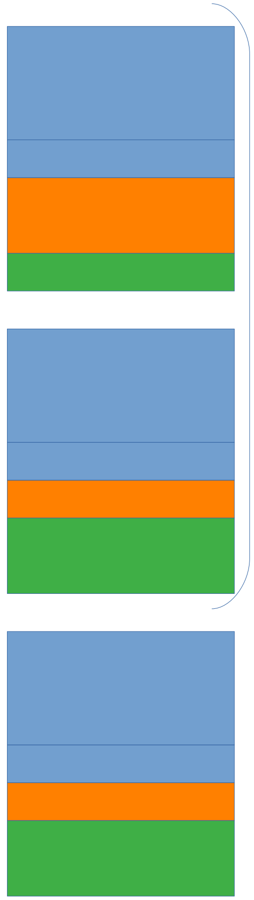

Inverse problem ?

Direct model

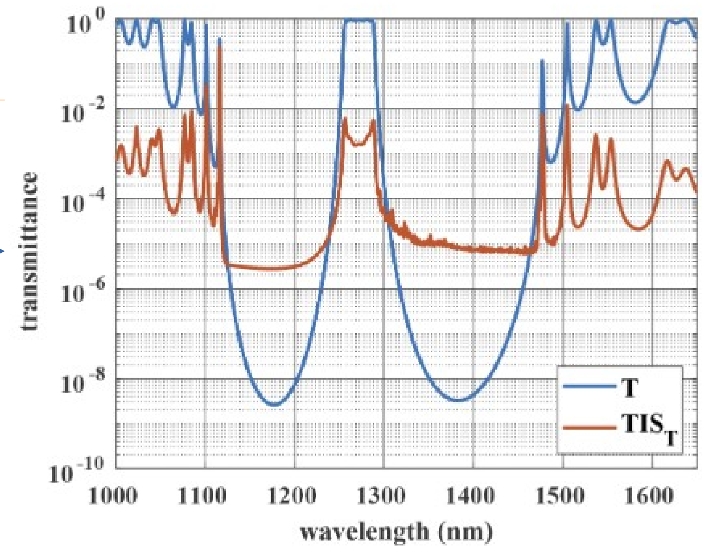

Multilayer optical thin film

Inverse Problems – **multi-layer design**

Predictor-designer Networks

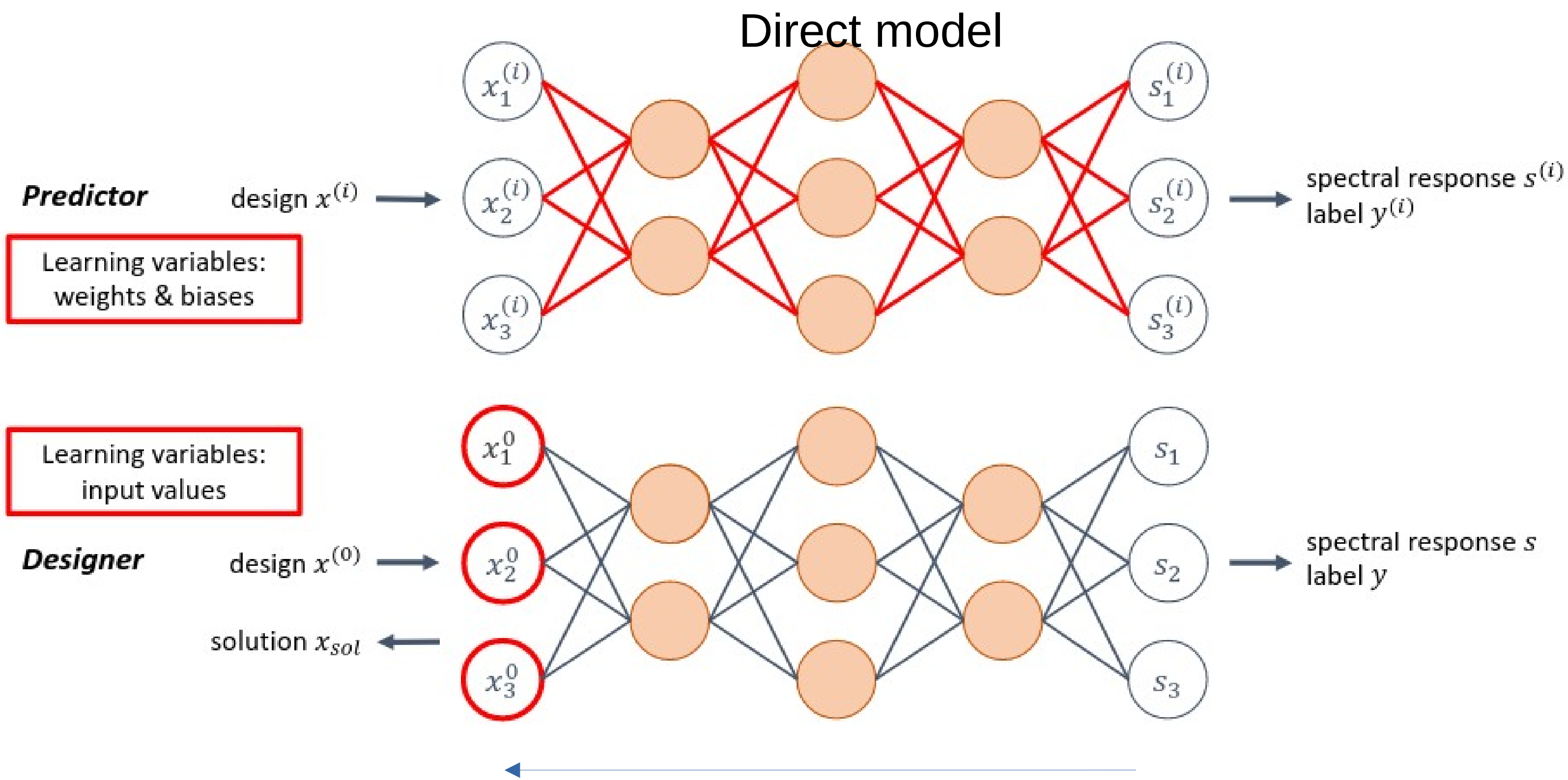

retro-propagate to modify the design

Predictor-Designer Networks: results

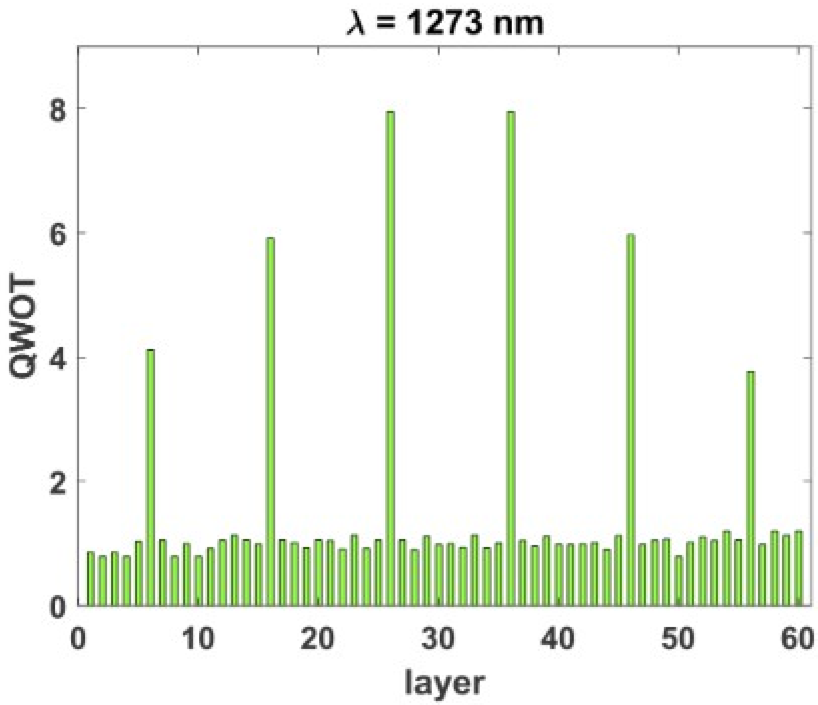

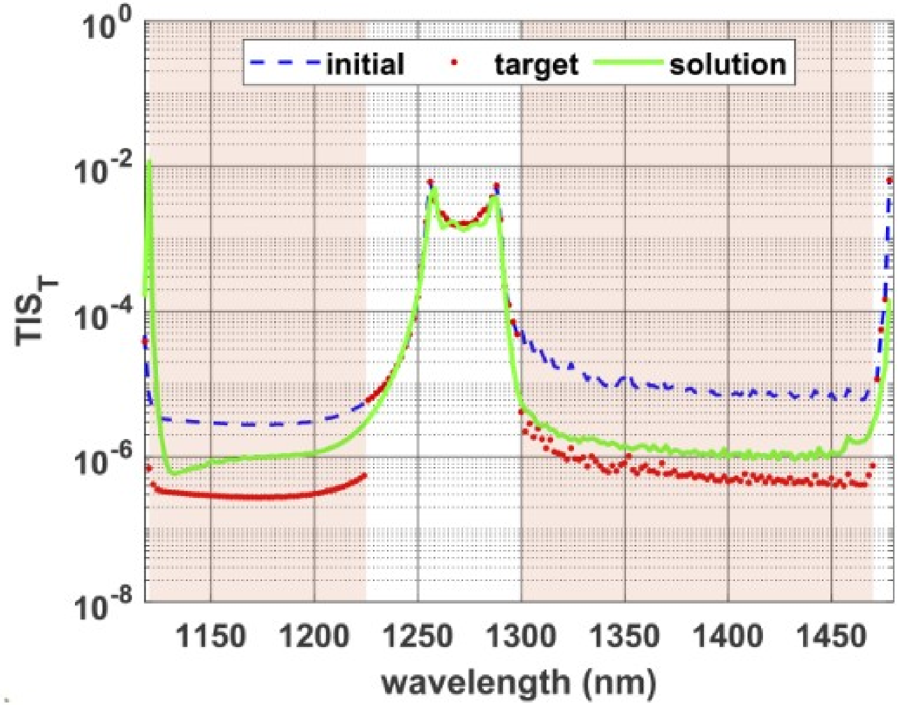

Partial conclusion :

- Inverse problem is addressed using neural networks
- Physics of the direct model is approximate by NN
- Inversion gives promising preliminary results

- main challenges : PINNS

Conclusion

- AI for image processing largely used

- AI approximation ability => approximate models in Physics

- collect datasets is still challenging

- Need to informed NN by Physics (PINNS) especially for inverse problems

Conclusion

- AI for image processing largely used

- AI approximation ability => approximate models in Physics

- collect datasets is still challenging

- Need to informed NN by Physics (PINNS) especially for inverse problems